

Entanglement signatures of a percolating quantum system

Subrata Pachhal^{1,*} and Adhip Agarwala^{1,†}

¹*Department of Physics, Indian Institute of Technology Kanpur, Kalyanpur, UP 208016, India*
(Dated: July 1, 2024)

Entanglement measures have emerged as one of the versatile probes to diagnose quantum phases and their transitions. Universal features in them expand their applicability to a range of systems, including those with quenched disorder. In this work, we show that when the underlying lattice has percolation disorder, free fermions at a finite density show interesting entanglement properties due to massively degenerate ground states. We define and calculate appropriate entanglement measures such as typical, annealed, and quenched entanglement entropy in both one and two dimensions, showing they can capture both geometrical aspects and electronic correlations of the percolated quantum system. In particular, while typical and annealed entanglement show volume law character directly dependent on the number of zero modes in the system, quenched entanglement is generally area law albeit showing characteristic signatures of the classical percolation transition. Our work presents an exotic interplay between the geometrical properties of a lattice and quantum entanglement in a many-body quantum system.

Introduction: Quantum entanglement [1, 2] and their measures [3–5] have established themselves as necessary tools to diagnose quantum phases and their transitions [6–16]. Moreover, the generalizations and extensions of bipartite entanglement entropy (EE) [3] including topological EE [17, 18], entanglement negativity [19–24], witnesses [25–28] and corner contributions [29–33] provide an encompassing framework to study quantum phases in and out of equilibrium. Their universal features at times make them indispensable to define unconventional quantum phases [34–38], particularly in the presence of disorder [39, 40]. Among disordered systems, percolation problems [41–43], where a lattice is probabilistically diluted either on the sites or bonds, are known to exhibit second-order phase transitions, namely geometrical phase transition, with universal critical exponents [43–47]. For instance, in the case of bond percolation if p is the probability of having a bond in the system such that $p = 1$ is a translationally invariant lattice then there exists a critical value of p known as the classical percolation threshold p_c , immediately below which the lattice gets geometrically disconnected [43]. Such geometrical phase transitions and their critical phenomena have been long studied in both classical and quantum systems [48–53] and recently in the context of topological phases [54–56]. However, the interplay of percolation disorder and entanglement properties has been little explored [57]. We visit entanglement measures in the light of percolation disorder in the simplest of fermionic quantum systems: free fermions hopping on a lattice. In particular, we address do entanglement measures show signatures of a geometrical phase transition? Do they still follow the usual area/volume law [58, 59] diagnostics?

In this work, we investigate the above questions to show that in percolating quantum systems, the conventional measures of bipartite entanglement entropy [60, 61]

have quite a few subtleties. The non-intuitive aspect of the results arises from massive exact degeneracy due to lattice percolation. In particular, we show that one needs to investigate different quantities: *typical* (S_{typ}), *annealed* (S_{ann}) and *quenched* EE (S_{quen}) each of which captures distinctive signatures. Interestingly, they often depend on the number of exact zero-modes (N_0) in the system, which is, in turn, related to the geometrical aspects of the lattice. We finally show that even the classical percolation threshold has footprints in quantum entanglement, where entanglement scaling depends on the emergent fractal nature of the largest cluster.

Measures of entanglement and free fermions: Given a wavefunction $|\psi\rangle$, or the density matrix ($\hat{\rho} = |\psi\rangle\langle\psi|$) of a system composed of two subsystems A and B , the EE of region A with B (or vice-versa) is given by $S_A = -\text{Tr}(\hat{\rho}_A \ln \hat{\rho}_A)$, where $\hat{\rho}_A = \text{Tr}_B \hat{\rho}$ is the reduced density matrix of the subsystem A . However, this definition assumes that the system is described by a unique wavefunction $|\psi\rangle$. But in the presence of degeneracies, it is more appropriate to study *typical* entanglement

$$S_{\text{typ}} = \langle S_A(\hat{\rho}_A) \rangle, \quad (1)$$

where the averaging is done over *pure* state ensembles made of degenerate wavefunctions [62, 63]. The wavefunction coefficients are complex and drawn from normal probability distributions implementing a uniform Haar measure over the unitary transformations about any reference state [64–67]. S_{typ} is however different from

$$S_{\text{ann}} = S_A(\langle \hat{\rho}_A \rangle), \quad (2)$$

where the averaging is done on the density matrix before evaluating its entanglement content. Such a measure we call *annealed* EE. In general $S_{\text{typ}} < S_{\text{ann}}$, since the latter reflects the maximum information content possible in a given Hilbert space consistent with Page’s result [62]. For instance, in a decoupled two spin system while S_A may seem to be zero, $S_{\text{typ}} \sim 0.33$, $S_{\text{ann}} = \ln 2$ (see Supplemental Material (SM) [68]).

* pachhal@iitk.ac.in

† adhip@iitk.ac.in

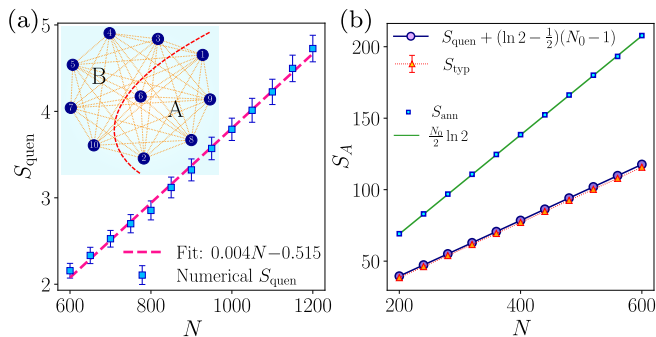


FIG. 1. **Zero dimensional model:** (a) S_{quen} (averaged over $N_C \equiv 10^3$ configurations) grows linearly with number of sites, N . (inset) Schematic of the model and subsystems A and B . (b) Behaviour of S_{typ} and S_{ann} with N . The number of zero-modes, $N_0 = N - 1$. Both are calculated using $N_R \equiv 10^4$ ensembles of random pure states.

In a many-body free fermionic system defined on N sites such that c_i^\dagger and c_i are the fermionic creation and annihilation operators, the ground state is often a unique Slater determinant and the bipartite entanglement is evaluated using the Peschel formulation of correlator matrix \mathcal{C} where its elements $c_{ij} = \langle c_i^\dagger c_j \rangle$ [60, 61]. However, the measure of typical and annealed entanglement becomes important for a system with ground state degeneracy. Thus, while for any single Slater determinant, the EE can be given by the corresponding correlator matrix $S(\mathcal{C}_A)$, when averaged over all choices of random wavefunction coefficients over the degenerate manifold, one gets $S_{\text{typ}} = \langle S(\mathcal{C}_A) \rangle$ and similarly $S_{\text{ann}} = S(\langle \mathcal{C}_A \rangle)$ (for an illustrative example of these quantities in a four-site toy model, see SM [68]). A simple way to break such exact degeneracies would be to add a small perturbative Anderson disorder $\eta \sim 10^{-12}$, which will choose a unique ground state. Then we define *quenched* entanglement, to capture the fermionic correlations in the system

$$S_{\text{quen}} = \langle S(\mathcal{C}_A) \rangle_\eta, \quad (3)$$

where the average is over disordered configurations. Before delving into percolation problems, we illustrate the role of these measures in a zero-dimensional system.

Zero-dimensional system: Consider a N site Hamiltonian where the fermions can hop from a site to any other site with strength $t = -1$ (see Fig. 1(a) inset) such that $H = -\sum_{i,j} c_i^\dagger c_j$. The single particle spectrum has one eigenvalue with energy $-N$, while $N - 1$ eigenvalues are exactly *zero*. A half-filled system here is thus $\binom{N-1}{2}$ fold degenerate. An infinitesimal η disorder of strength $\eta = 10^{-12}$ can be added in form of a term $\sum_i \epsilon_i c_i^\dagger c_i$ where $\epsilon \in [-\eta, \eta]$ to break this exact degeneracy. Given the long-range character of hopping, the entanglement content for equal bipartition of the system such that $N_A = N/2$ is still volume law where $S_{\text{quen}} = s_v N + s_0$ with a coefficient $s_v \sim 0.004$ as shown in Fig. 1(a). However, when such massive degeneracy is

intact, reflects in

$$S_{\text{typ}} = S_{\text{quen}} + (\ln 2 - \frac{1}{2})(N_0 - 1), \quad (4)$$

where the second term arises from the effective geometrical component because of $N_0 = N - 1$ number of zero-modes of the system (see Fig. 1(b)). The factor of $(\ln 2 - \frac{1}{2})$ arises from the effective random pure states made out of N_0 zero-modes [69]. In general, when the number of occupied zero-modes is fN_0 ($0 < f < 1$), the geometrical volume law is empirically proportional to $f(1-f)$ representing the effective phase space volume (see SM [68]). Another alternate measure of the entanglement in this system is to average the correlator matrix first. For such a system at half-filling, while $c_{ii} = \frac{1}{2}$ and $c_{ij} = \frac{1}{2N}$ [70] leading to $S_{\text{ann}} \sim \frac{N_0}{2} \ln 2$.

While it may appear that all three entanglement measures are volume law and therefore similar, it is pertinent to emphasize that they all have different physical content. While S_{quen} captures the fermionic correlations, which are inherently volume law since the network is zero-dimensional, the character of S_{typ} and S_{ann} capture the massive degeneracy of the system - where S_{typ} measures the average bipartite EE for any choice of a typical *pure* state, S_{ann} measures the maximal subsystem entanglement when the complete system itself becomes *mixed* due to averaging of the correlator matrix. For instance, the entanglement measure of the full system has $S_{\text{ann}} \neq 0$ but $S_{\text{typ}} = 0$. In general, when a complete system of interest takes a mixed character various other entanglement measures have been found to isolate quantum correlations between its partitions such as mutual information [71–73], entanglement negativity [19–24] and witnesses [25–28]. Having discussed the subtleties and the different measures of entanglement, we now discuss quantum percolation problems, where studying these various measures of entanglement becomes indispensable given spectral degeneracies.

One-dimensional percolation: We first discuss percolation in a one-dimensional lattice, where spinless fermions hop with the following tight-binding Hamiltonian

$$H = -t \sum_{i=1}^L \left(c_i^\dagger c_{i+1} + \text{h.c.} \right), \quad (5)$$

where L is the system size and $t = 1$. The probability of having a bond is given by p such that at $p = 0$, the system contains a completely decoupled set of sites, while at $p = 1$ it is a translationally invariant fermionic chain (see Fig. 2(a)). The percolation transition, where one end of the lattice gets connected to the other end, happens at $p = p_c = 1$ [45, 74]. The fermion filling is kept fixed at $= 1/2$. Given the Hamiltonian is real and has a sublattice symmetry, it belongs to the BDI symmetry class [75, 76], which is retained under the percolation protocol.

The fermionic ground state describes a Fermi sea at $p = 1$; however, at any $p < 1$, given the fermions reside on disconnected clusters, the ground state should be

interpreted as an Anderson insulator state. This is consistent with the effect of any uncorrelated disorder in one dimension [77, 78]. The entanglement content, therefore, is generically expected to be $\sim \ln L$ at $p = 1$ and $\mathcal{O}(1)$ in presence of disorder, as is known from Cardy-Calabrese result for critical states [10, 12, 79] and area law entanglement for short-range correlated states [14, 58]. At any p given the presence of disconnected clusters, there are spectral degeneracies that can be split using an infinitesimal disorder η to obtain S_{quen} (see Fig. 2(b)). An analytical estimate can be obtained as follows. Given P_s is the probability of having a s sized cluster, in general, its maximal entanglement content in equal bipartition is $(\frac{c}{6} \ln(\frac{s}{\pi}) + c_0)$ [10] where c is the central charge ($c = 1$) of the one-dimensional bosonic CFT and c_0 is an area law piece. Thus for a thermodynamic system,

$$\tilde{S}_{\text{quen}} = \sum_{s=2}^{\infty} P_s \left(\frac{c}{6} \ln\left(\frac{s}{\pi}\right) + c_0 \right) \quad (6)$$

where \tilde{S}_{quen} represents a configuration averaged value over S_{quen} . Here $P_s = s n_s = s(1-p)^2 p^{s-1}$ which, given any p , is the probability that an arbitrary site of the diluted chain belongs to a cluster of s number of sites [43]. n_s is the mean number of clusters of size s . This has a linear rise at small p and a divergence near $p = 1$. This analytic behavior, along with our numerical results, is shown in Fig. 2(b) (here, $c_0 = 0.409 \pm 0.002$). Broadly, the behavior indeed remains area law (with a p dependent coefficient) except at $p = 1$ where the logarithmic L dependence is restored. Interestingly, the average cluster size $\langle M \rangle = \sum_s s P_s$, diverges near $p \rightarrow p_c$ as $(p_c - p)^{-\gamma}$ with $\gamma = 1$ [43]. Thus $\tilde{S}_{\text{quen}} \sim \frac{c}{6} \ln \langle M \rangle \sim \frac{c}{6} \ln \xi^{\frac{1}{\nu}}$, where the geometric correlation length ξ also diverges as $(p_c - p)^{-\nu}$ with $\nu = 1$ [43]. Since at $p = 1$, $\xi \sim L$, one expects a scaling where, $e^{6\tilde{S}_{\text{quen}}} L^{-\frac{\gamma}{\nu}} \sim 1$ which is shown in Fig. 2(c). Thus, the entanglement measure captures the percolation exponents near the geometrical phase transition here at $p_c = 1$. However, as discussed before, these results required us to put an infinitesimal degeneracy splitting disorder η , which also breaks the symmetry of the full Hamiltonian. Without any such disorder, the massive degenerate manifold of zero-modes leads to geometrical components of EE, as we discuss next.

As the one-dimensional lattice is percolated, various clusters of different sizes appear on the chain. For any odd s the cluster has one single particle zero energy mode. Thus, the zero-mode density is,

$$\frac{N_0}{L} = \sum_{m=0}^{\infty} n_{2m+1} = \frac{1-p}{1+p}, \quad (7)$$

for a L sized chain at percolation probability p . This analytical behavior and the disorder averaged numerical estimate of zero-modes number \tilde{N}_0 are shown in Fig. 2(e). A half-filled state in such a system again leads to highly degenerate many-body eigenspace. A uniform Haar mea-

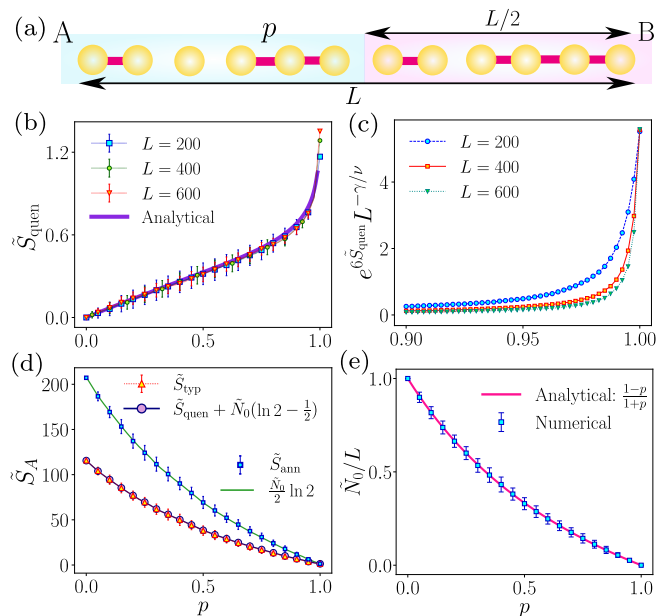


FIG. 2. **Bond diluted chain:** (a) Subsystems A and B in a L sized chain, with bond occupation probability p . (b) \tilde{S}_{quen} with p for different values of L (c) Scaling of \tilde{S}_{quen} near $p = p_c = 1$ with $\gamma = \nu = 1$. (d) Behaviour of \tilde{S}_{typ} and \tilde{S}_{ann} with p (e) Zero-mode density ($\equiv \tilde{N}_0/L$) for $L = 600$ compared to analytical result [80]. In (b), (c), and (e) $N_C = 10^3$, in (d) $N_C = 40$ and for each configuration, $N_R = 10^2$.

sure here leads to

$$\tilde{S}_{\text{typ}} = \tilde{S}_{\text{quen}} + \left(\ln 2 - \frac{1}{2}\right) \tilde{N}_0, \quad (8)$$

while $\tilde{S}_{\text{ann}} \sim \frac{\tilde{N}_0}{2} \ln 2$. All the behaviors match the numerical results as shown in Fig. 2(d). Interestingly, the mutual information between the two subsystems removes this large volume law contribution and shows a rise similar to \tilde{S}_{quen} , only near $p = 1$ when the lattice gets connected (see SM [68]). Thus, geometrical disorder, as in one-dimensional percolation, provides distinctive signatures in various entanglement measures both from intra-cluster fermionic correlations and from geometric components of the lattice itself.

Two-dimensional percolation: In two dimensional percolation the system has a finite p_c ; for instance in square lattice bond percolation it is known $p_c = \frac{1}{2}$ [81–83]. At $p = p_c$ a spanning cluster develops with critical exponent $\gamma = 43/18$ [43]. We again pose the question of different entanglement measures for this system. As is known that for a two-dimensional free fermionic system - any infinitesimal disorder localizes all the wavefunctions [77, 78], thus in terms of electronic properties, we expect the system to be localized for all values of p [84–87] even though there have been studies finding numerical evidence otherwise [88–94]. Given any p the mean number of clusters containing k bonds, n_k is given by $n_k = \sum_t g(k, t) p^k (1-p)^t$ where t is the perimeter

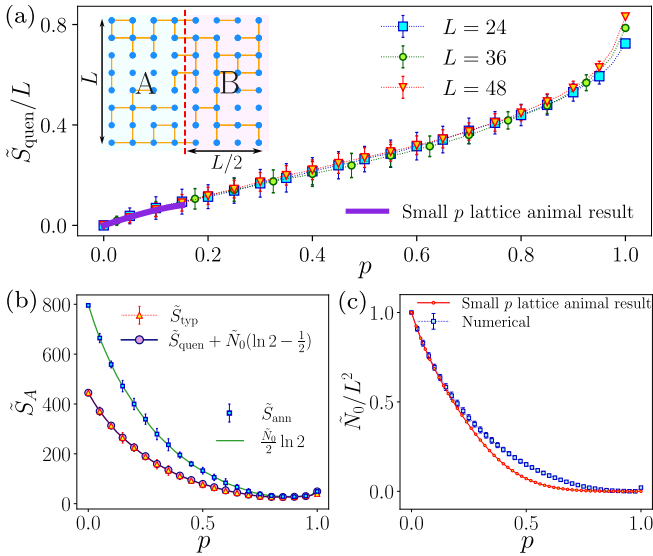


FIG. 3. **Bond diluted square lattice:** (a) \tilde{S}_{quen} with p for different system sizes. ($N_C = 10^2$). (inset) Schematic of a configuration with A and B partitions. (b) \tilde{S}_{typ} and \tilde{S}_{ann} with p . $N_C = 10, N_R = 10^2$ (c) \tilde{N}_0 with p ($N_C = 10^2$), compared to lattice animal results (see text). In (b-c), $L = 48$.

of the cluster and $g(k, t)$ is the geometrical factor associated with the number of lattice animals given (k, t) [95]. Since any square lattice is a bipartite graph with a symmetric spectrum, the E_F remains pinned to zero at half-filling even under percolation. We find that S_{quen} follows an area law behavior (see Fig. 3(a)) i.e. $\propto L$ for $p < 1$. While at $p = 1$, the complete square lattice is restored, leading to a finite Fermi sea, the entanglement is $\sim L \ln L$ given by the Widom conjecture [12, 96]. At $p < 1$, however, such a momentum space description is no longer applicable. At small p , one can enumerate the lattice animals exactly and count their entanglement contribution, as shown by the analytical curve in Fig. 3(a) (for details, see SM [68]). This is in contrast to S_{typ} and S_{ann} , which again depend on the extensive number of zero-modes present in the system (see Fig. 3(b)). The density of zero-modes can be estimated analytically from lattice animals, given by

$$\frac{N_0}{L^2} = \sum_{k,t} n_0(k, t) g(k, t) p^k (1-p)^t, \quad (9)$$

where $n_0(k, t)$ is the number of zero-modes in a cluster of bond-size k and perimeter t . A lower bound on N_0 , calculated using lattice animals up to $k = 4$, is shown in Fig. 3(c), and it matches well with disorder averaged zero-mode number \tilde{N}_0 for small p values (details in SM [68]). Given the zero-modes really appear from the geometrical aspects of the clusters, it is thus imperative that they also determine the entanglement content.

To distill any signature of percolation transition at $p = p_c$, we calculate the configuration averaged quenched bipartite EE of the *largest* cluster ($\equiv S_{\text{quen}}^{lc}$) as a function

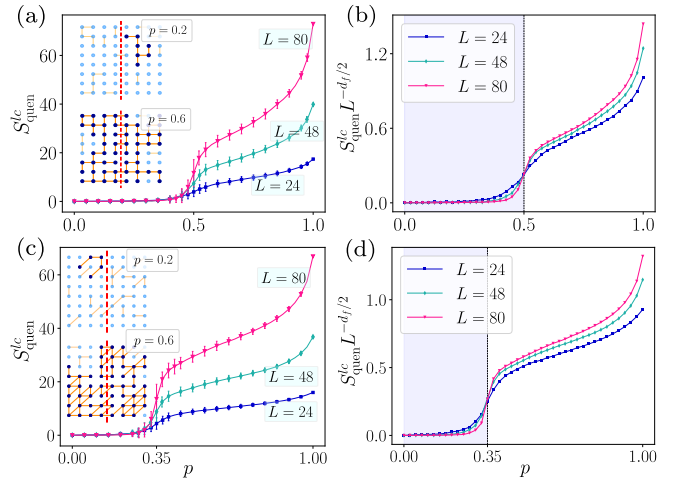


FIG. 4. **Largest cluster:** (a) Disorder averaged S_{quen}^{lc} with p , for square lattice of different size L ($N_C = 10^2$). (insets) typical configurations for two values of p where *dark-blue* sites form the largest cluster. (b) Scaling of S_{quen}^{lc} with the fractal dimension $d_f = 91/48$ shows crossing at percolation threshold $p_c = 0.5$. In (c-d) similar to (a-b) but for triangular lattice with $p_c \sim 0.35$ (see text).

of p and show this in Fig. 4(a). Interestingly, while for $p < p_c$ $S_{\text{quen}}^{lc} \propto L^0$, for $p > p_c$ $S_{\text{quen}}^{lc} \propto L$ where L is the linear dimension of the lattice. Given it is known that the largest cluster follows a scaling L^{d_f} [43] where d_f is the fractal dimension of the system, for a typical area law behavior, we expect $S_{\text{quen}}^{lc} \propto L^{d_f/2}$ near p_c . A scaling collapse using this form shows a crossing (see Fig. 4(b)) at $p = p_c = 0.5$ with, $d_f = 91/48$ as known for two-dimensional percolation transition. Since this physics should be independent of the microscopic lattice, we apply the same analysis to a tight-binding triangular lattice (Fig. 4(c)). Again, the same collapse shows a crossing (Fig. 4(d)) near $p = p_c = 2 \sin(\frac{\pi}{18})$ [82] illustrating that the entanglement scaling indeed follows the universal features of geometrical phase transitions even though the exact value of p_c is itself not universal.

Outlook: Quantum entanglement and its measures have taken a defining role in deciphering the nature of quantum phases. In particular, the nature of low-energy excitations are often equated with whether the bipartite EE follows area law or has logarithmic corrections. In this work, we revisit various measures of quantum entanglement in the context of percolation disorder in free fermionic lattice Hamiltonians. We find that percolation disorder inherently generates extensive degeneracies, which gives rise to subtleties in standard bipartite EE. It is then important to either break the massive degeneracies by putting infinitesimal disorder which leads to the S_{quen} , or otherwise investigate quantities such as S_{typ} and S_{ann} which includes physics of the degenerate manifold. We uncover that such measures have contributions from both fermionic correlations and geometrical aspects. While S_{quen} generically follow area law, S_{typ} and S_{ann} are

volume law in character. These quantities can, in turn, be estimated from the properties of the clusters, which either cut the entanglement bipartition or contribute to the zero-mode degeneracies. Interestingly, the entanglement measure of the largest cluster can capture even the classical percolation threshold in two dimensions. While we have restricted our investigation to three quantities S_{typ} , S_{ann} and S_{quen} , it would be worthwhile to quantify the amount of classical and quantum correlations in these systems. In physical systems where a perturbative quenched disorder is inherent, it is expected that S_{quen} represents a more meaningfully observable quantity than S_{typ} . Similarly, given in estimation of S_{ann} complete density matrix is averaged, the annealed EE contains both classical and quantum correlations. In this context, quantities such as mutual information and entanglement negativity may be of interest.

While in this work, we do not propose any experimental setups to measure such entanglement signatures, find-

ing realistic proposals [16, 97–99] in this direction would be interesting to pursue. Similarly, we have focused in this study exclusively on bipartite EE, given its relevance to quantum condensed matter systems. Various other measures have been pursued in quantum information to investigate phases and phase transitions [100, 101]. A comprehensive investigation of these, in regard to percolation disorder, is another prospective study. Finally, investigating this physics in both symmetry-protected topological systems and topologically ordered systems will be an exciting future direction.

Acknowledgement: We acknowledge fruitful discussions with Diptarka Das, Apratim Kaviraj, Saikat Ghosh, G. Sreejith, Saikat Mondal, and Harish Adsule. S.P. acknowledges funding from IIT Kanpur Institute Fellowship. AA acknowledges support from IITK Initiation Grant (IITK/PHY/2022010). Numerical calculations were performed on the workstation *Wigner* at IITK.

-
- [1] A. Einstein, B. Podolsky, and N. Rosen, Can quantum-mechanical description of physical reality be considered complete?, *Phys. Rev.* **47**, 777 (1935).
 - [2] R. Horodecki, P. Horodecki, M. Horodecki, and K. Horodecki, Quantum entanglement, *Rev. Mod. Phys.* **81**, 865 (2009).
 - [3] C. H. Bennett, H. J. Bernstein, S. Popescu, and B. Schumacher, Concentrating partial entanglement by local operations, *Phys. Rev. A* **53**, 2046 (1996).
 - [4] M. B. Plenio and S. Virmani, An introduction to entanglement measures., *Quantum Inf. Comput.* **7**, 1 (2007).
 - [5] L. Amico, R. Fazio, A. Osterloh, and V. Vedral, Entanglement in many-body systems, *Rev. Mod. Phys.* **80**, 517 (2008).
 - [6] T. J. Osborne and M. A. Nielsen, Entanglement in a simple quantum phase transition, *Phys. Rev. A* **66**, 032110 (2002).
 - [7] A. Osterloh, L. Amico, G. Falci, and R. Fazio, Scaling of entanglement close to a quantum phase transition, *Nature* **416**, 608 (2002).
 - [8] G. Vidal, J. I. Latorre, E. Rico, and A. Kitaev, Entanglement in quantum critical phenomena, *Phys. Rev. Lett.* **90**, 227902 (2003).
 - [9] G. Refael and J. E. Moore, Entanglement entropy of random quantum critical points in one dimension, *Phys. Rev. Lett.* **93**, 260602 (2004).
 - [10] P. Calabrese and J. Cardy, Entanglement entropy and quantum field theory, *Journal of Statistical Mechanics: Theory and Experiment* **2004**, P06002 (2004).
 - [11] A. Hama, R. Ionicioiu, and P. Zanardi, Bipartite entanglement and entropic boundary law in lattice spin systems, *Phys. Rev. A* **71**, 022315 (2005).
 - [12] D. Gioev and I. Klich, Entanglement entropy of fermions in any dimension and the widom conjecture, *Phys. Rev. Lett.* **96**, 100503 (2006).
 - [13] T. Barthel, M.-C. Chung, and U. Schollwöck, Entanglement scaling in critical two-dimensional fermionic and bosonic systems, *Phys. Rev. A* **74**, 022329 (2006).
 - [14] M. B. Hastings, An area law for one-dimensional quantum systems, *Journal of Statistical Mechanics: Theory and Experiment* **2007**, P08024 (2007).
 - [15] I. Mondragon-Shem, M. Khan, and T. L. Hughes, Characterizing disordered fermion systems using the momentum-space entanglement spectrum, *Phys. Rev. Lett.* **110**, 046806 (2013).
 - [16] G. A. Canella and V. V. França, Superfluid-insulator transition unambiguously detected by entanglement in one-dimensional disordered superfluids, *Scientific reports* **9**, 15313 (2019).
 - [17] A. Kitaev and J. Preskill, Topological entanglement entropy, *Phys. Rev. Lett.* **96**, 110404 (2006).
 - [18] M. Levin and X.-G. Wen, Detecting topological order in a ground state wave function, *Phys. Rev. Lett.* **96**, 110405 (2006).
 - [19] M. Horodecki, P. Horodecki, and R. Horodecki, Separability of mixed states: necessary and sufficient conditions, *Physics Letters A* **223**, 1 (1996).
 - [20] G. Vidal and R. F. Werner, Computable measure of entanglement, *Phys. Rev. A* **65**, 032314 (2002).
 - [21] H. Shapourian, K. Shiozaki, and S. Ryu, Partial time-reversal transformation and entanglement negativity in fermionic systems, *Phys. Rev. B* **95**, 165101 (2017).
 - [22] H. Shapourian, P. Ruggiero, S. Ryu, and P. Calabrese, Twisted and untwisted negativity spectrum of free fermions, *SciPost Phys.* **7**, 037 (2019).
 - [23] H. Shapourian, S. Liu, J. Kudler-Flam, and A. Vishwanath, Entanglement negativity spectrum of random mixed states: A diagrammatic approach, *PRX Quantum* **2**, 030347 (2021).
 - [24] G. Parez and W. Witczak-Krempa, Entanglement negativity between separated regions in quantum critical systems, *Phys. Rev. Res.* **6**, 023125 (2024).
 - [25] M. Lewenstein, B. Kraus, P. Horodecki, and J. I. Cirac, Characterization of separable states and entanglement witnesses, *Phys. Rev. A* **63**, 044304 (2001).
 - [26] B. M. Terhal, Detecting quantum entanglement, *Theoretical Computer Science* **287**, 313 (2002), natural Computing.

- [27] M. Žnidarič, T. Prosen, G. Benenti, and G. Casati, Detecting entanglement of random states with an entanglement witness, *Journal of Physics A: Mathematical and Theoretical* **40**, 13787 (2007).
- [28] F. Iglói and G. Tóth, Entanglement witnesses in the xy chain: Thermal equilibrium and postquench nonequilibrium states, *Phys. Rev. Res.* **5**, 013158 (2023).
- [29] E. Fradkin and J. E. Moore, Entanglement entropy of 2d conformal quantum critical points: Hearing the shape of a quantum drum, *Phys. Rev. Lett.* **97**, 050404 (2006).
- [30] H. Casini and M. Huerta, Universal terms for the entanglement entropy in 2+1 dimensions, *Nuclear Physics B* **764**, 183 (2007).
- [31] P. Bueno, R. C. Myers, and W. Witczak-Krempa, Universality of corner entanglement in conformal field theories, *Phys. Rev. Lett.* **115**, 021602 (2015).
- [32] J. Helmes, L. E. Hayward Sierens, A. Chandran, W. Witczak-Krempa, and R. G. Melko, Universal corner entanglement of dirac fermions and gapless bosons from the continuum to the lattice, *Phys. Rev. B* **94**, 125142 (2016).
- [33] J. D’Emidio, R. Orús, N. Laflorencie, and F. de Juan, Universal features of entanglement entropy in the honeycomb hubbard model, *Phys. Rev. Lett.* **132**, 076502 (2024).
- [34] H. Li and F. D. M. Haldane, Entanglement spectrum as a generalization of entanglement entropy: Identification of topological order in non-abelian fractional quantum hall effect states, *Phys. Rev. Lett.* **101**, 010504 (2008).
- [35] L. Fidkowski, Entanglement spectrum of topological insulators and superconductors, *Phys. Rev. Lett.* **104**, 130502 (2010).
- [36] A. M. Turner, F. Pollmann, and E. Berg, Topological phases of one-dimensional fermions: An entanglement point of view, *Phys. Rev. B* **83**, 075102 (2011).
- [37] J. Cho and K. W. Kim, Quantum phase transition and entanglement in topological quantum wires, *Scientific reports* **7**, 2745 (2017).
- [38] S. Mondal, S. Bandyopadhyay, S. Bhattacharjee, and A. Dutta, Detecting topological phase transitions through entanglement between disconnected partitions in a kitaev chain with long-range interactions, *Phys. Rev. B* **105**, 085106 (2022).
- [39] E. Prodan, T. L. Hughes, and B. A. Bernevig, Entanglement spectrum of a disordered topological chern insulator, *Phys. Rev. Lett.* **105**, 115501 (2010).
- [40] Z. Liu and R. N. Bhatt, Quantum entanglement as a diagnostic of phase transitions in disordered fractional quantum hall liquids, *Phys. Rev. Lett.* **117**, 206801 (2016).
- [41] S. R. Broadbent and J. M. Hammersley, Percolation processes: I. crystals and mazes, *Mathematical Proceedings of the Cambridge Philosophical Society* **53**, 629–641 (1957).
- [42] J. W. Essam, Reports on progress in physics, *Percolation theory* **43**, 833 (1980).
- [43] D. Stauffer and A. Aharony, *Introduction to percolation theory* (Taylor and Francis, 1992).
- [44] R. G. Priest and T. C. Lubensky, Critical properties of two tensor models with application to the percolation problem, *Phys. Rev. B* **13**, 4159 (1976).
- [45] P. J. Reynolds, H. E. Stanley, and W. Klein, Ghost fields, pair connectedness, and scaling: exact results in one-dimensional percolation, *Journal of Physics A: Mathematical and General* **10**, L203 (1977).
- [46] H. Kesten, Scaling relations for 2 D-percolation, *Communications in Mathematical Physics* **109**, 109 (1987).
- [47] M. Sahimi, *Encyclopedia of Complexity and Systems Science*, edited by R. A. Meyers (Springer New York, New York, NY, 2009) pp. 6538–6545.
- [48] R. Balian, R. Maynard, and G. rard Toulouse, *Ill-condensed matter*, Vol. 31 (World Scientific, 1979).
- [49] D. S. Fisher, Random transverse field ising spin chains, *Phys. Rev. Lett.* **69**, 534 (1992).
- [50] D. S. Fisher, Phase transitions and singularities in random quantum systems, *Physica A: Statistical Mechanics and its Applications* **263**, 222 (1999), proceedings of the 20th IUPAP International Conference on Statistical Physics.
- [51] A. Dutta, Quantum spin glass with long-range random interactions, *Phys. Rev. B* **65**, 224427 (2002).
- [52] A. K. Sen, K. K. Bardhan, and B. K. Chakrabarti, *Quantum and semi-classical percolation and breakdown in disordered solids*, Vol. 762 (Springer, 2009).
- [53] I. A. Kovács, Quantum multicritical point in the two- and three-dimensional random transverse-field ising model, *Phys. Rev. Res.* **4**, 013072 (2022).
- [54] I. Sahlberg, A. Westström, K. Pöyhönen, and T. Ojanen, Topological phase transitions in glassy quantum matter, *Phys. Rev. Res.* **2**, 013053 (2020).
- [55] M. N. Ivaki, I. Sahlberg, and T. Ojanen, Criticality in amorphous topological matter: Beyond the universal scaling paradigm, *Phys. Rev. Res.* **2**, 043301 (2020).
- [56] S. Mondal, S. Pachhal, and A. Agarwala, Percolation transition in a topological phase, *Phys. Rev. B* **108**, L220201 (2023).
- [57] L. Gong and P. Tong, Localization-delocalization transitions in a two-dimensional quantum percolation model: von neumann entropy studies, *Phys. Rev. B* **80**, 174205 (2009).
- [58] J. Eisert, M. Cramer, and M. B. Plenio, Colloquium: Area laws for the entanglement entropy, *Rev. Mod. Phys.* **82**, 277 (2010).
- [59] W. Li, L. Ding, R. Yu, T. Roscilde, and S. Haas, Scaling behavior of entanglement in two- and three-dimensional free-fermion systems, *Phys. Rev. B* **74**, 073103 (2006).
- [60] I. Peschel, Calculation of reduced density matrices from correlation functions, *Journal of Physics A: Mathematical and General* **36**, L205 (2003).
- [61] I. Peschel and V. Eisler, Reduced density matrices and entanglement entropy in free lattice models, *Journal of Physics A: Mathematical and Theoretical* **42**, 504003 (2009).
- [62] D. N. Page, Average entropy of a subsystem, *Phys. Rev. Lett.* **71**, 1291 (1993).
- [63] E. Bianchi, L. Hackl, M. Kieburg, M. Rigol, and L. Vidmar, Volume-law entanglement entropy of typical pure quantum states, *PRX Quantum* **3**, 030201 (2022).
- [64] I. Bengtsson and K. Życzkowski, *Geometry of Quantum States: An Introduction to Quantum Entanglement* (Cambridge University Press, 2017).
- [65] C. Nadal, S. N. Majumdar, and M. Vergassola, Statistical distribution of quantum entanglement for a random bipartite state, *Journal of Statistical Physics* **142**, 403 (2011).
- [66] O. C. Dahlsten, C. Lupo, S. Mancini, and A. Serafini, Entanglement typicality, *Journal of Physics A: Mathe-*

- mathematical and Theoretical **47**, 363001 (2014).
- [67] G. Biswas, A. Biswas, and U. Sen, Inhibition of spread of typical bipartite and genuine multiparty entanglement in response to disorder, *New Journal of Physics* **23**, 113042 (2021).
- [68] See supplemental material for additional details on toy examples, zero-dimensional model, mutual information in one dimension and results from lattice animals.
- [69] Y. Liu, J. Kudler-Flam, and K. Kawabata, Symmetry classification of typical quantum entanglement, *Phys. Rev. B* **108**, 085109 (2023).
- [70] G. Gori, S. Paganelli, A. Sharma, P. Sodano, and A. Trombettoni, Explicit hamiltonians inducing volume law for entanglement entropy in fermionic lattices, *Phys. Rev. B* **91**, 245138 (2015).
- [71] C. Adami and N. J. Cerf, von neumann capacity of noisy quantum channels, *Phys. Rev. A* **56**, 3470 (1997).
- [72] B. Groisman, S. Popescu, and A. Winter, Quantum, classical, and total amount of correlations in a quantum state, *Phys. Rev. A* **72**, 032317 (2005).
- [73] M. M. Wolf, F. Verstraete, M. B. Hastings, and J. I. Cirac, Area laws in quantum systems: Mutual information and correlations, *Phys. Rev. Lett.* **100**, 070502 (2008).
- [74] P. J. Reynolds, H. E. Stanley, and W. Klein, A real-space renormalization group for site and bond percolation, *Journal of Physics C: Solid State Physics* **10**, L167 (1977).
- [75] A. Altland and M. R. Zirnbauer, Nonstandard symmetry classes in mesoscopic normal-superconducting hybrid structures, *Phys. Rev. B* **55**, 1142 (1997).
- [76] A. Agarwala, A. Haldar, and V. B. Shenoy, The tenfold way redux: Fermionic systems with n-body interactions, *Annals of Physics* **385**, 469 (2017).
- [77] P. W. Anderson, Absence of diffusion in certain random lattices, *Phys. Rev.* **109**, 1492 (1958).
- [78] E. Abrahams, P. W. Anderson, D. C. Licciardello, and T. V. Ramakrishnan, Scaling theory of localization: Absence of quantum diffusion in two dimensions, *Phys. Rev. Lett.* **42**, 673 (1979).
- [79] M. M. Wolf, Violation of the entropic area law for fermions, *Phys. Rev. Lett.* **96**, 010404 (2006).
- [80] Numerically, we always associate zero-modes with states lying in the energy gap $\Delta E \sim 10^{-14}$ around $E = 0$.
- [81] M. F. Sykes and J. W. Essam, Some exact critical percolation probabilities for bond and site problems in two dimensions, *Phys. Rev. Lett.* **10**, 3 (1963).
- [82] M. F. Sykes and J. W. Essam, Exact critical percolation probabilities for site and bond problems in two dimensions, *Journal of Mathematical Physics* **5**, 1117 (1964).
- [83] H. Kesten, The critical probability of bond percolation on the square lattice equals $\frac{1}{2}$, *Communications in Mathematical Physics* **74**, 41 (1980).
- [84] S. Kirkpatrick and T. P. Eggarter, Localized states of a binary alloy, *Phys. Rev. B* **6**, 3598 (1972).
- [85] R. Raghavan and D. C. Mattis, Eigenfunction localization in dilute lattices of various dimensionalities, *Phys. Rev. B* **23**, 4791 (1981).
- [86] Y. Shapir, A. Aharony, and A. B. Harris, Localization and quantum percolation, *Phys. Rev. Lett.* **49**, 486 (1982).
- [87] C. M. Soukoulis and G. S. Grest, Localization in two-dimensional quantum percolation, *Phys. Rev. B* **44**, 4685 (1991).
- [88] V. Srivastava and M. Chaturvedi, New scaling results in quantum percolation, *Phys. Rev. B* **30**, 2238 (1984).
- [89] T. Koslowski and W. von Niessen, Mobility edges for the quantum percolation problem in two and three dimensions, *Phys. Rev. B* **42**, 10342 (1990).
- [90] H. N. Nazareno, P. E. de Brito, and E. S. Rodrigues, Quantum percolation in a two-dimensional finite binary alloy: Interplay between the strength of disorder and alloy composition, *Phys. Rev. B* **66**, 012205 (2002).
- [91] M. F. Islam and H. Nakanishi, Localization-delocalization transition in a two-dimensional quantum percolation model, *Phys. Rev. E* **77**, 061109 (2008).
- [92] G. Schubert and H. Fehske, Dynamical aspects of two-dimensional quantum percolation, *Phys. Rev. B* **77**, 245130 (2008).
- [93] B. S. Dillon and H. Nakanishi, Localization phase diagram of two-dimensional quantum percolation, *The European Physical Journal B* **87**, 1 (2014).
- [94] G. De Tomasi, O. Hart, C. Glittum, and C. Castelnovo, Effects of critical correlations on quantum percolation in two dimensions, *Phys. Rev. B* **105**, 224316 (2022).
- [95] M. F. Sykes, D. S. Gaunt, and M. Glen, Perimeter polynomials for bond percolation processes, *Journal of Physics A: Mathematical and General* **14**, 287 (1981).
- [96] B. Swingle, Entanglement entropy and the fermi surface, *Phys. Rev. Lett.* **105**, 050502 (2010).
- [97] R. Islam, R. Ma, P. M. Preiss, M. Eric Tai, A. Lukin, M. Rispoli, and M. Greiner, Measuring entanglement entropy in a quantum many-body system, *Nature* **528**, 77 (2015).
- [98] A. M. Kaufman, M. E. Tai, A. Lukin, M. Rispoli, R. Schittko, P. M. Preiss, and M. Greiner, Quantum thermalization through entanglement in an isolated many-body system, *Science* **353**, 794 (2016).
- [99] A. Lukin, M. Rispoli, R. Schittko, M. E. Tai, A. M. Kaufman, S. Choi, V. Khemani, J. Léonard, and M. Greiner, Probing entanglement in a many-body-localized system, *Science* **364**, 256 (2019).
- [100] B. Zeng, X. Chen, D.-L. Zhou, X.-G. Wen, *et al.*, *Quantum information meets quantum matter* (Springer, 2019).
- [101] G. D. Chiara and A. Sanpera, Genuine quantum correlations in quantum many-body systems: a review of recent progress, *Reports on Progress in Physics* **81**, 074002 (2018).

Supplemental Material to “Entanglement signatures of a percolating quantum system”

I. Entanglement between two free spins

To understand the notion of *typical* and *annealed* entanglement in contrast with standard bipartite entanglement entropy, let us consider two free spins A and B as shown in Fig. S5(a). A general choice of the valid many-body wavefunction of the system will be,

$$|\psi\rangle = a|\downarrow_A\downarrow_B\rangle + b|\downarrow_A\uparrow_B\rangle + c|\uparrow_A\downarrow_B\rangle + d|\uparrow_A\uparrow_B\rangle, \quad (\text{S1})$$

since the spins are free. Given the wavefunction coefficients (here a, b, c and d) are complex random variables chosen from a Gaussian distribution with zero mean and unit variance, the random state $|\psi\rangle$ can be thought of as Haar uniform pure state [64, 65]. So, in a general form, any random pure state of our free spin system can be written as,

$$|\psi\rangle = \sum_{i,j} \phi_{i,j} |\alpha_A^i\rangle \otimes |\alpha_B^j\rangle, \quad (\text{S2})$$

with $\alpha^i, \alpha^j \in \{\uparrow, \downarrow\}$ is the basis of the Hilbert space and wavefunction coefficients $\phi_{i,j}$ s (i.e. a, b, c, d) are the elements of a Gaussian random matrix Φ , satisfying the wavefunction normalisation constraint $\sum_{i,j} |\phi_{i,j}|^2 = |a|^2 + |b|^2 + |c|^2 + |d|^2 = 1$. Now, the partial density matrix for the spin A will be,

$$\begin{aligned} \hat{\rho}_A &= \text{Tr}_B(\hat{\rho}) = \text{Tr}_B(|\psi\rangle\langle\psi|) \\ &= \sum_m \langle\alpha_B^m| \left(\sum_{i,j} \sum_{k,l} \phi_{i,j} \phi_{k,l}^* |\alpha_A^i\rangle\langle\alpha_A^k| \otimes |\alpha_B^j\rangle\langle\alpha_B^l| \right) |\alpha_B^m\rangle \\ &= \sum_{i,k} \sum_m \phi_{i,m} \phi_{k,m}^* |\alpha_A^i\rangle\langle\alpha_A^k| \\ &= \sum_{i,k} \chi_{i,k} |\alpha_A^i\rangle\langle\alpha_A^k|, \end{aligned} \quad (\text{S3})$$

where $\chi_{i,k} = \sum_m \phi_{i,m} \phi_{k,m}^*$ is the matrix element of $\Phi\Phi^\dagger$, consequently $\hat{\rho}_A = \Phi\Phi^\dagger$ in the basis of α_A . From this, it is straightforward to see in our system,

$$\hat{\rho}_A = \begin{pmatrix} |a|^2 + |b|^2 & ac^* + bd^* \\ ca^* + db^* & |c|^2 + |d|^2 \end{pmatrix}. \quad (\text{S4})$$

Now using, $\hat{\rho}_A$ one can numerically calculate bipartite entanglement entropy $S_A(\hat{\rho}_A) = \text{Tr}(\hat{\rho}_A \ln \hat{\rho}_A)$ and average it over numerous Gaussian ensembles of wavefunction coefficients $\{a, b, c, d\}$ to find *typical* entanglement measure $S_{\text{typ}} = \langle S_A(\hat{\rho}_A) \rangle \simeq 0.33$. We also define *annealed* entanglement as $S_{\text{ann}} = S_A(\langle \hat{\rho}_A \rangle) = \text{Tr}(\langle \hat{\rho}_A \rangle \ln \langle \hat{\rho}_A \rangle)$. To calculate this, one first takes ensemble averaged (this average is also taken over wavefunction coefficients as described earlier) partial density matrix $\langle \hat{\rho}_A \rangle$ which turns out to be $\frac{1}{2}I_2$ here, and then find entanglement entropy to get $S_{\text{ann}} = \ln 2$.

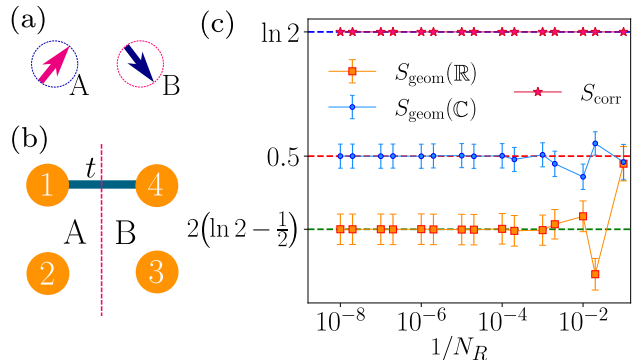


FIG. S5. (a) Two free spin A and B . (b) A four-site toy model with only two sites (1 and 4) are connected via fermionic hopping of strength t . The bipartition used for entanglement calculation is shown in red-dashed line. (c) Different contributions in S_{typ} for the four-site toy example. Contribution from fermionic correlation S_{corr} is always $\ln 2$. For complex random coefficients, the geometric contribution S_{geom} converges to $S_{\text{geom}}(\mathbb{C}) = \frac{1}{2}$ with increasing N_R (number of random pure state ensembles), and for real choices it converges to $S_{\text{geom}}(\mathbb{R}) = (2 \ln 2 - 1)$.

II. Four site fermionic toy example

To illustrate how *typicality* in entanglement measure appears in a fermionic model, consider the system where two spinless fermions hops (with hopping strength $t = -1$) on a four-site structure as shown in Fig. S5(b). While the single-particle spectrum is straight-forwardly given by $\{\pm 1, 0, 0\}$, the many-body ground state is not unique but two-fold degenerate. This can be seen because, to minimize the energy, while one fermion resides in a delocalized state between sites 1 and 4, another fermion can be on either site 2 or 3. The two valid ground-state wavefunctions of the system are

$$|\Psi_1\rangle = \frac{1}{\sqrt{2}}(c_1^\dagger + c_4^\dagger)c_2^\dagger|\Omega\rangle, \quad (\text{S5})$$

$$|\Psi_2\rangle = \frac{1}{\sqrt{2}}(c_1^\dagger + c_4^\dagger)c_3^\dagger|\Omega\rangle, \quad (\text{S6})$$

where $|\Omega\rangle$ is the fermionic vacuum and the entanglement entropy across the partition is clearly $\ln 2$ given the delocalized fermion. However, any general wavefunction of the form

$$|\Psi\rangle = \phi_1|\Psi_1\rangle + \phi_2|\Psi_2\rangle, \quad (\text{S7})$$

is also a valid wave function of the system. Given the coefficients are randomly drawn from a Gaussian distribution and follow wavefunction normalization constraint, they form a random pure state similar to what we discussed in I. This leads to similar considerations of *typical*

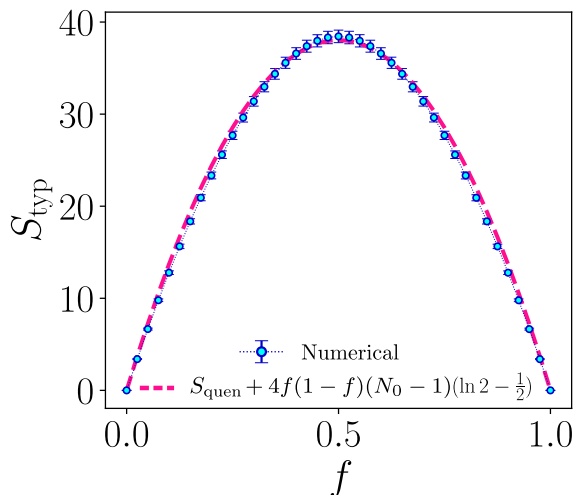


FIG. S6. S_{typ} as a function of filling f , for the zero-dimensional fermionic problem. Numerical data is calculated for a system of $N = 200$ sites with equal bipartition and averaged over 10^4 ensembles of random pure states.

entanglement S_{typ} as described in the main text. However, now it has components arising from the fermionic correlations within the connected cluster across the partition (the delocalized state between site 1 and 4) and contributions due to a random choice of coefficients ϕ_1 and ϕ_2 . In general,

$$S_{\text{typ}} = S_{\text{corr}} + S_{\text{geom}}, \quad (\text{S8})$$

where S_{corr} captures the fermionic correlations in connected regions and S_{geom} arises out of typicality due to degeneracy, often arising out of disconnected sites. Therefore, the latter has information about the geometrical properties of the network. In the present example, while $S_{\text{corr}} = \ln 2$, S_{geom} depends on the choices of the wavefunction coefficients (ϕ_1 and ϕ_2) used in the formation of random pure states, leading to the symmetry classification of the typical entanglement [69]. In class A [75], the coefficients are complex, and the analytical result shows $S_{\text{geom}}(\mathbb{C}) = \frac{1}{2}$, while in class AI [75] where the coefficients are real, it is evaluated to be $S_{\text{geom}}(\mathbb{R}) = (2 \ln 2 - 1)$. In Fig. S5(c), we show that our numerical results converge towards analytical results with the increasing number of pure ensembles (N_R) used in the calculation of S_{typ} .

III. Zero-dimensional fermionic problem

An all-to-all connected fermionic hopping network hosts $N_0 = N - 1$ number of zero energy states for a N site system. So, a typical many-body wavefunction of the system will be a random pure state made out of these degenerate zero energy states. Here, we choose the wavefunction coefficients to be real, restricting it to class AI [69]. Now, S_{typ} at half filling $f = \frac{1}{2}$, and for equal bipar-

tion, typical entanglement contains a small fermionic correlation part and a substantial geometric contribution because of the massive degeneracy in the spectrum. While the geometric part follows the symmetry classification result [69], the fermionic part is captured in S_{quen} , evaluated using the degeneracy breaking protocol as discussed in the main text. Now, for any general filling f ($0 < f < 1$) with equal bipartition, the available phase space volume is $f(1-f)$; consequently, the effective degenerate Hilbert space dimension becomes $\sim 2^{af(1-f)N_0}$, where a is a dimensionless constant. Then, using Page's result [62], we empirically find the typical entanglement in the leading order to be,

$$S_{\text{typ}}(f) = S_{\text{quen}}(f) + 4f(1-f)(N_0 - 1)\left(\ln 2 - \frac{1}{2}\right), \quad (\text{S9})$$

so that it remains consistent with the result at half filling ($S_{\text{typ}} = S_{\text{quen}} + (N_0 - 1)\left(\ln 2 - \frac{1}{2}\right)$). In Fig. S6, we show the numerical values as a function of filling (f), which match well with our empirical formula.

IV. Mutual information in one-dimensional percolation

In general, mutual information (MI) is a good measure of entanglement between two subsystems A and B when the full system is in mixed state [71]. Since finding annealed entanglement entropy (S_{ann}) in our study is associated with the mixedness of the full system, here we intend to show the behavior of MI in the percolated tight-binding chain. With the same bipartition protocol used in the main text, MI between A and B is,

$$I_{A:B} = S_{\text{ann}}^A + S_{\text{ann}}^B - S_{\text{ann}}^{AB}, \quad (\text{S10})$$

where, the annealed entanglement entropy of the full system $S_{\text{ann}}^{AB} \neq 0$ due to mixed character of the correlator matrix for the full system at half filling. In Fig. S7, the behavior of disorder averaged MI ($\tilde{I}_{A:B}$) with bond occupation probability p is shown for our one-dimensional percolation model. In $p \rightarrow 0$ limit, $S_{\text{ann}}^A + S_{\text{ann}}^B \approx S_{\text{ann}}^{AB}$. While the behavior shows reduction of large volume law (due to zero modes) contribution in S_{ann} for small p values, a sharp rise appears near the classical percolation threshold $p = p_c = 1$, where the lattice gets connected. This is similar to \tilde{S}_{quen} (see Fig. S7), which is expected because, after the removal of zero mode contribution, only the electronic correlation part reflects in MI.

V. Lattice animals, their entanglement and number of zero modes

In the case of square lattice percolation, the quenched entanglement S_{quen} can be captured using the lattice animals and their contributions to entanglement given a bipartition. For a lattice animal of bond size k (i.e., the

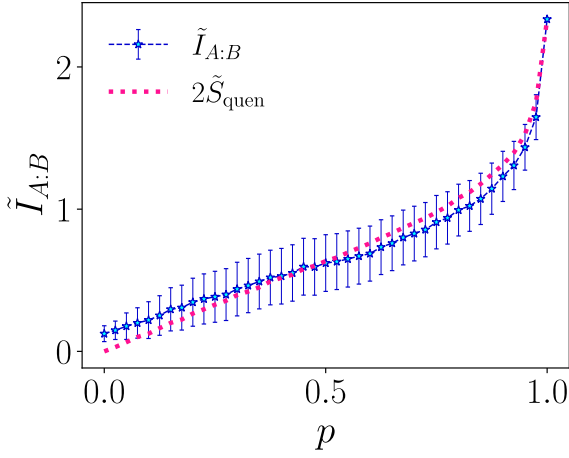


FIG. S7. Disorder averaged MI $\tilde{I}_{A:B}$ with percolation probability p for the free fermionic chain of length $L = 200$. The bipartition protocol is the same as the main text. The disorder average is taken over 500 configurations, and for each configuration, 10^3 random pure states are chosen for averaging the correlator matrix. Note the similarity in behaviour with \tilde{S}_{quen} (same data as shown in the main text for $L = 200$).

number of bonds) and perimeter t , we calculate the bipartite entanglement entropy S_{animal}^b with the partition dissecting the animal in a certain way. Now if P_{animal}^b is the probability that the different animals of the same $\{k, t\}$ appear on that given partition and give rise to the same S_{animal}^b , then for a square lattice of linear size L ,

$$S_{\text{quen}} \approx \sum_{\text{animal}, b} P_{\text{animal}}^b S_{\text{animal}}^b L. \quad (\text{S11})$$

The factor of L comes because there are L number of sites on the partition where the animal can appear.

Similarly, we calculate the number of zero energy modes in the percolating square lattice using lattice animal enumeration. The mean number of bond clusters is given by $g(k, t)p^k(1-p)^t$ and $g(k, t)$ is the number of lattice animals of size $\{k, t\}$ [95]. Then the number of zeromodes for L sized system is,

$$N_0 = \sum_{k, t} n_0(k, t)g(k, t)p^k(1-p)^t L^2, \quad (\text{S12})$$

where $n_0(k, t)$ is the number of zeromodes in a cluster of size $\{k, t\}$. For small values of k (up to 4) and t (up to 12), all these data are tabulated in TABLE I. Now, using eqn. (S11) and eqn. (S12), one can calculate quenched entanglement and the number of zeromodes in the percolated square lattices. Since these small-sized clusters are dominant in small values of percolation probability p , our result from TABLE I matches the disorder averaged numerical results (\tilde{S}_{quen} and \tilde{N}_0) at small p values (see main text).

Animals	S_{animal}^b	P_{animal}^b	k, t	$g(k, t)$	$n_0(k, t)$
	0	q^4	0, 4	1	1
	$\ln 2$	pq^6	1, 6	2	0
	0.56234...	$6p^2q^8$	2, 8	6	1
	$\ln 2$	$14p^3q^{10}$	3, 10	14	0
	0.41328...	$p^3(7q^{10} + 2q^9)$			
	0.45056...	$6p^3q^{10}$	3, 10	4	1
	1.17903...	$2p^3q^9$	3, 9	4	0
	0.54387...	$p^4(34q^{12} + 8q^{11})$	4, 12	54	1
	0.56234...	$p^4(20q^{12} + 8q^{11})$			
	$\ln 2$	$6p^4q^{12}$			
	1.14317...	$2p^4q^{12}$	4, 12	54	1
	1.17349...	$8p^4q^{11}$	4, 11	32	1
	0.95494...	$8p^4q^{11}$			
	0.32346...	$p^4(10q^{12} + 8q^{11})$	4, 11	32	1
	0.63651...	$p^4(30q^{12} + 8q^{11})$	4, 11	32	1
	0.37677...	$2p^4q^{12}$	4, 12	1	3
	0.83299...	p^4q^8	4, 8	1	2

TABLE I. Small-sized lattice animals (up to bond-size $k = 4$ and perimeter $t = 12$) and their contribution in quenched entanglement S_{quen} and number of zeromodes N_0 for percolated square lattice. S_{animal}^b is the entanglement of a lattice animal given the bipartition cuts the animal in a certain way, and P_{animal}^b is the probability of that animal appears on that bipartition. The prefactors in P_{animal}^b are decided by the number of animal structures with the same partition, giving the same S_{animal}^b . For a given $\{k, t\}$, $g(k, t)$ is the number of lattice animals, and $n_0(k, t)$ is the number of zero energy states they can host.